23nd IAHR International Symposium on Ice

Ann Arbor, Michigan USA, May 31 to June 3, 2016

The influence of ice structure on thermo-elastic waves in saline ice

Aleksey Marchenko[1,2], Andrii Murdza[1], Ben Lishman[3],
[1]*The University Centre in Svalbard, Longyearbyen, Norway*
[2]*Sustainable Arctic Marine and Coastal Technology (SAMCoT), Centre for Research-based Innovations (CRI), Norwegian University of Science and Technology, Trondheim, Norway*
[3]*Portsmouth University, Department of Engineering, UK*
Aleksey.Marchenko@unis.no
Andrii.Murdza@unis.no
Ben.Lishman@port.ac.uk

We formulate a structural model of saline ice and describe a model solution describing the propagation of thermo-elastic waves. Thermo-elastic waves are excited by periodical oscillations of the ice surface temperature. The properties of these thermo-elastic waves are determined by the mean ice temperature (background temperature), the ice salinity and the amount of liquid brine trapped in closed brine pockets. Results from an experiment, measuring thermo-elastic waves in ice, performed in the UNIS cold laboratory, are described. The characteristics of these thermo-elastic waves are compared with the theory. It is shown that amount of liquid brine trapped in closed brine pockets is an important variable in describing how the ice deforms under oscillating background temperature.

1. Introduction

Saline ice is made up of a matrix of solid frozen H_2O, containing pockets and channels filled with a mixture of salty brine and gas. The structure and composition of saline ice can change under mechanical and thermal loads: for example, when ice is cooled, liquid freezes to form ice, this freezing process ejects salt, and so the remaining brine may become saltier. Many properties of ice, including thermal properties, may therefore depend on the distribution of brine, and on the movement of the brine. The extent to which brine can migrate through the ice is controlled by the permeability of the ice. Weeks and Ackley (1986) proposed that sea ice is impermeable when brine content is less than 5%, and permeable otherwise. More recent work suggests that sea ice always contains porous channels (Golden et al., 2007). Permeability depends temperature, since channels can open and close through melting and freezing. Further, permeability depends on not just the present state of the ice, but on the historical evolution of temperature and salt fluxes at its boundaries.

The first model of thermal expansion of sea ice was proposed by Malmgren (1927). This model assumes constant salinity in the sample, so that phase changes (from ice to brine and vice versa), which lead to local density changes (since water is more dense than ice), can have global effects on the density and hence on the thermal expansion. A later model, proposed by Cox (1983), assumes that when phase changes occur, brine is expelled from (or impelled into) the ice, and thus phase changes have no effect on the thermal expansion. These two models rely on two different assumptions about permeability, with Malmgren assuming sea ice is impermeable to brine, and Cox assuming that the ice matrix offers no resistance to brine migration. Johnson and Metzner (1990) measured the linear thermal expansion of cylindrical ice samples taken from first year congelation sea ice in Harrison Bay, Alaska, and found evidence to support Cox's model of unconstrained brine migration.

It is evident that Cox's assumption contradicts the conclusion of Weeks and Ackley (1986) when the liquid brine content of saline ice is less than 5%. Golden et al. (2007) discovered increasing fractional connectivity of the brine inclusions in saline ice with increasing temperature, but mentioned that some part of brine could exist in closed pockets even when the liquid brine content is greater than 5%. Recent measurements of the thermally induced deformations of saline ice samples performed with Fiber Bragg strain and temperature sensors confirmed this conclusion (Marchenko et al, 2016). Experimentally registered deformations of saline ice samples caused by temperature changes were different from fresh ice samples. The difference was explained by the existence of closed brine pockets. The fraction of the total brine contained in these closed pockets varies depending on the temperature.

A model of saline ice assuming that some fraction of the liquid brine is trapped in closed brine pockets, and the remainder of the liquid brine exists in permeable channels, was formulated by Marchenko and Lishman (2015). A model solution describing thermo-elastic waves in saline ice was formulated and investigated. In the present paper we formulate a structural model of saline ice, describe new experiments on the measurement of thermo-elastic waves at the surface of saline ice samples, analyze the results obtained from the experiments and compare them with the theory.

2. Structural model of saline ice

Saline ice consists of both pure ice surrounding closed brine pockets (ICP) and liquid brine in permeable channels (BPC). The saline ice density is determined by the formula

$$\rho_{si} = \rho_{icp} \nu_{icp} + \rho_b \nu_b , \qquad [1]$$

where ρ_{icp} and ρ_b are the densities of the ICP and BPC, and ν_{icp} and ν_b are the volumetric concentrations of the ICP and BPC respectively. They must therefore sum to 1 (since the entire system is composed of either ICP or BPC):

$$\nu_{icp} + \nu_b = 1 . \qquad [2]$$

The volumetric concentrations of pure ice and liquid brine in closed pockets in the ICP are denoted as ν_i and ν_{bi} respectively ($\nu_i + \nu_{bi} = 1$). We assume typical sea ice composition, such that $\nu_b << 1$ and $\nu_{bi} << 1$.

The ICP salinity is a constant

$$\sigma_{icp} = const . \qquad [3]$$

It is assumed that the liquid brine and the pure ice are in thermodynamic equilibrium. Therefore the salinities of brine in closed pockets and in permeable channels are the same, and so the volumetric concentration of liquid brine in the ICP is calculated by the formula

$$\nu_{bi} = \frac{\rho_{icp} \sigma_{icp}}{\rho_b \sigma_b} , \qquad [4]$$

where σ_b is the brine salinity. The salinity of sea ice is determined by the formula

$$\rho_{si} \sigma_{si} = \rho_{icp} \nu_{icp} \sigma_{icp} + \rho_b \nu_b \sigma_b . \qquad [5]$$

Using the definition of sea ice density (1) we find that the volumetric concentration of the ICP is calculated as

$$\nu_{icp} = \frac{\rho_{icp} (\sigma_{si} - \sigma_{icp})}{\rho_{icp} (\sigma_{si} - \sigma_{icp}) + \rho_b (\sigma_b - \sigma_{si})} . \qquad [6]$$

The brine density ρ_b is calculated with the formula (Schwerdtfeger, 1963)

$$\rho_b = \rho_w (1 + S) , \qquad [7]$$

where ρ_w=1000 kg/m^3 is the water density and S is the fractional salt content of the brine. The brine salinity is calculated from the condition of thermodynamic equilibrium

$$\sigma_b = \frac{S}{1+S};\ S = -0.0182 \cdot T,\ T > -8.2^\circ\,\mathrm{C};$$
$$S = 0.149 - 0.01 \cdot (T + 8.2),\ T \in (-23^\circ\mathrm{C}, -8.2^\circ\mathrm{C}). \quad [8]$$

Pure ice density depends on the temperature according to the formula

$$\rho_i \approx \frac{916.8}{1+\alpha_i T}(\mathrm{kg/m^3}), \quad [9]$$

where α_i=1.58·10^{-4}K^{-1} is the volumetric coefficient of thermal expansion of pure ice.

The ICP density is calculated with the formula (Schwerdtfeger, 1963)

$$\rho_{icp} = \frac{\rho_b \rho_i \sigma_b}{\rho_i \sigma_{icp} + \rho_b (\sigma_b - \sigma_{icp})}. \quad [10]$$

The volumetric coefficient of thermal expansion of the ICP is calculated by the formula

$$\alpha_{icp} = -\frac{1}{\rho_{icp}} \frac{d\rho_{icp}}{dT}. \quad [11]$$

3. Thermo-elastic waves in saline ice

Periodical temperature oscillations at the surface of a solid material filling the half-space x<0 penetrate inside the material as thermal waves. Temperature oscillations are described inside the material by the formula (see, e.g., Landau and Lifshitz, 1988)

$$\delta T = A_T \exp(ikx + i\omega t), \quad [12]$$

where A_T is the temperature amplitude, and ω and k are the wave frequency and wave number. The dispersion equation gives a rule for the calculation of the wave number when the wave frequency is known:

$$\omega = ik^2(\lambda / \rho c). \quad [13]$$

Here ρ, λ and c are the density, the thermal conductivity and the specific heat capacity of the material.

Thermal waves are accompanied by elastic deformations when the material has thermo-elastic properties. In this case thermal waves become thermo-elastic waves. Since saline ice includes liquid brine then thermo-elastic waves in saline ice are accompanied by the phase changes and brine migration. The dispersion equation of thermo-elastic waves in saline ice is written in the form (Marchenko and Lishman, 2015)

$$\omega = ik^2 / X_T\,,\ X_T\lambda_{si0} = \left\langle \rho c \right\rangle_{si0} + \rho_{i0} L_i(\alpha_{\nu b} + \nu_{icp0}\alpha_{\nu bi})\,, \qquad [14]$$

$$\alpha_{\nu b} = -\frac{\nu_{b0}\sigma_{b0,T}}{\sigma_{b0}},\ \alpha_{\nu bi} = -\left(\frac{\rho_b\sigma_b}{\rho_{icp}}\right)_{0,T}\left(\frac{\rho_{icp}\nu_{bi}}{\rho_b\sigma_b}\right)_0,$$

where the subscript "0" means that the value of the quantity is equal to a background value. The coefficients of specific heat capacity and thermal conductivity are calculated by the formulas

$$\left\langle \rho c \right\rangle_{si} = \rho_i c_i \nu_i \nu_{icp} + \rho_b c_b(\nu_b + \nu_{bi}\nu_{icp})\,,\ \lambda_{si} = \lambda_i \nu_i \nu_{icp} + \lambda_b(\nu_b + \nu_{bi}\nu_{icp})\,, \qquad [15]$$

where c_i and c_b are the specific heat capacities, and λ_i and λ_b are the thermal conductivities of ice and brine, L_i=333.4 kJ/kg is the latent heat of ice.

It is assumed that the specific heat capacity and thermal conductivity of brine are equal to the specific heat capacity and thermal conductivity of water. The specific heat capacities and thermal conductivities of ice and water are given by the formulas

$$c_w = 4.23\,\text{kJ/(kg}^\circ\text{C)}\,,\ c_i = 2.12\,\text{kJ/(kg}^\circ\text{C)}\,,\ \lambda_w = 0.58\,\text{W/(m}^\circ\text{C)}\,,\ \lambda_i = 2.24\,\text{W/(m}^\circ\text{C)}\,. \qquad [16]$$

The amplitude of vertical displacement of the ice surface is calculated with the formula

$$A_u = \omega A_T \alpha_{vix}\,. \qquad [17]$$
$$\alpha_{vix} = \alpha_e \omega / k\,,\ \alpha_e = (\rho_{b0,T}\nu_{b0} + \gamma_{b0}\alpha_{icp0}\mathrm{K}X_T)/\Delta\,,\ \gamma_{b0} = \rho_{b0}k_{si,b0}/\mu_b\,,$$
$$\Delta = \gamma_{b0}(4\mu/3 + \mathrm{K})X_T - (\rho_b\sigma_b)_0\,,$$

where μ_b=1.8·10^{-3} Pa·s is the dynamic viscosity of water, μ = 3.8 GPa and K = 8.8 GPa are the shear modulus and the bulk modulus of sea ice, and the permeability of saline ice by brine is determined by the formula

$$k_{si,b} = k_{si,b0}e^{15\sqrt{\nu_b}}\ , \qquad [18]$$

where the coefficient $k_{si,b0}$=10^{-13} m^2 characterizes ice permeability at low values of the liquid brine content (Zhu et al, 2006).

The amplitudes A_u (the amplitude of the vertical displacement of the ice surface) and A_T (the amplitude of the temperature variation) can be measured in experiments. Their absolute ratio $|A_u/A_T|$ (the DT ratio) depends on the ice characteristics and wave frequency. The model given can be adapted to describe experimental data by varying the background characteristics ν_{b0} and ν_{bi0}. The ice permeability $k_{si,b0}$ can also be used as a validation parameter since it is not well known. Theoretical dependencies of the DT ratio on the mean ice temperature are shown in Fig.1a when closed brine pockets are absent (σ_{icp}=0) and in Fig.1b when the permeable brine channels are absent (σ_{icp}=σ_{si}). The values of ice salinity σ_{si} are shown in the figures. One can see

that the DT ratios shown in Fig.1a are much smaller than those shown in Fig.1b. This is the same as saying that temperature oscillations cause larger deformations when the brine cannot migrate than when all brine can freely migrate, and therefore illustrates the discrepancy between Malmgren's model and Cox's model as discussed in our introduction. In the case when the closed brine pockets and the permeable brine channels are both present, the dependence of the DT ratio on mean ice temperature follows the shape of Fig. 1a at low temperatures and Fig. 1b at high temperatures. From formula (17) it follows that

$$A_u / A_T > 0,\ \sigma_{icp} = 0;\ A_u / A_T < 0,\ \sigma_{si} = \sigma_{icp}. \qquad [19]$$

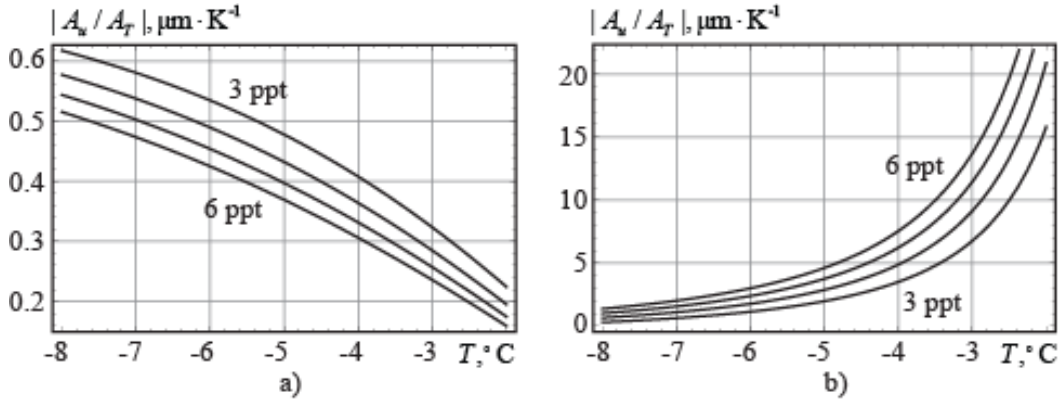

Figure 1. Theoretical dependencies of the DT ratio from the temperature calculated for saline ice without closed brine pockets (a) and for saline ice without permeable brine channels (b). The dependencies are constructed for the ice salinities 3, 4, 5 and 6 ppt.

4. Experimental investigation of thermo-elastic waves

Experiments to measure thermo-elastic waves were undertaken in the UNIS cold laboratory in October 2015. Saline ice samples were prepared from a mixture of sea water and fresh water. Toroidal samples were frozen by adding saline water, layer by layer, into a cylindrical plastic vessel with a fixed coaxial vertical pipe inside. Fiber optic strain and temperature sensors (FBG sensors) were used to measure lengthening of the samples in the vertical direction. The fiber was fixed by steel plates and bolts on the top and the bottom of the ice sample, as shown in Fig. 2. The FBG thermistor was placed near the FBG strain sensor. The ice torus was insulated from the environment by foam plastic (Fig 3a).

The upper surface of the torus was subjected to periodical variations of air temperature, caused by the cycle of the fans in the cold laboratory. The period of the air temperature variations was 12 minutes. The wave number is calculated using the dispersion equation derived by Marchenko and Lishman (2015). The inverse wavenumber k^{-1}, with a wave period of 12 minutes, is around 1cm. This quantity characterizes the depth of penetration of the air temperature fluctuations into the ice. The FBG strain sensor recorded the vertical deformation of the ice torus $\varepsilon=\Delta L/L$, where $L\approx$25cm is the vertical dimension of the torus and ΔL is the variation of L due to the thermal action. The sampling frequency was 1 Hz. The air temperature was registered less than 1cm from the ice surface with a Testo 176T4 rod-probe, and on the ice surface with a Testo 176T4 wire-probe (Fig. 3).

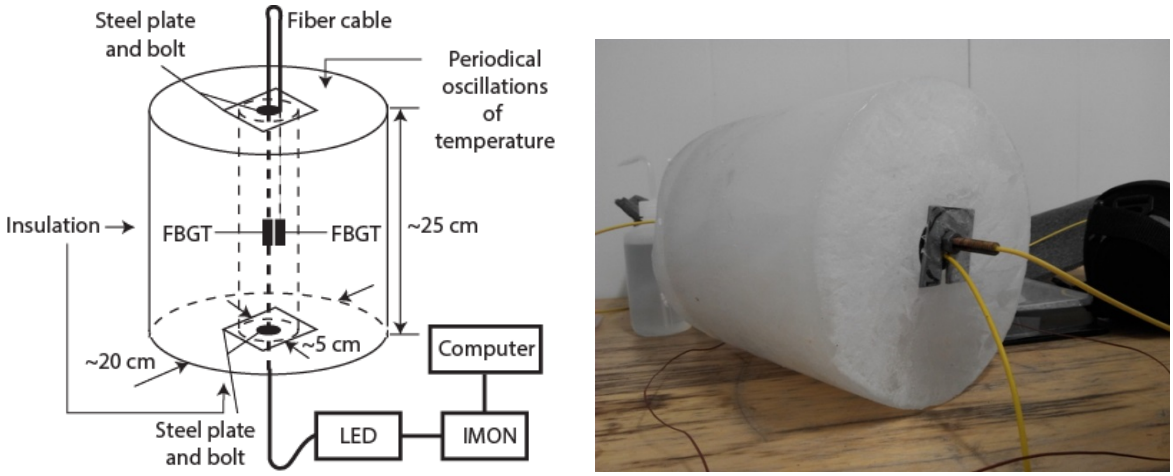

a) b)

Figure 2. Schematic of experiment for detection of thermo-elastic waves (a). Ice sample with optical fiber (b).

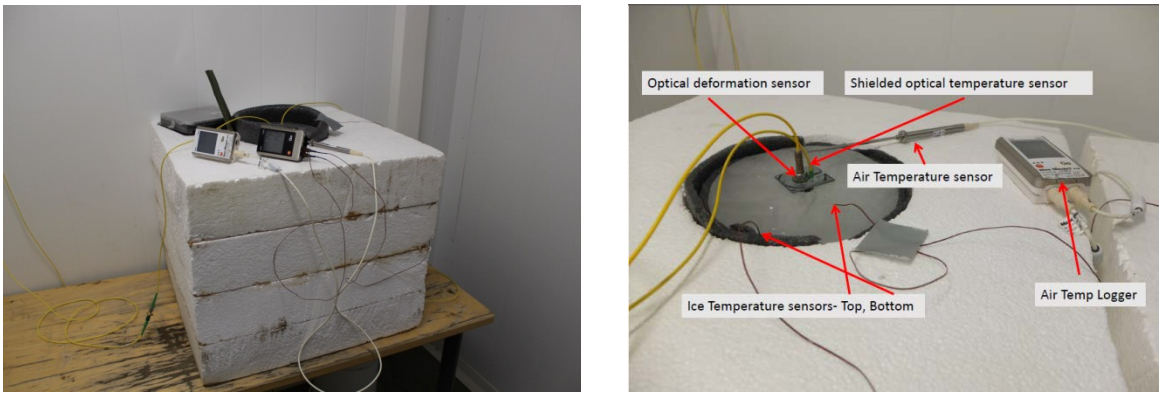

a) b)

Figure 3. Photos of full experiment (a) and sensor installed on the sample (b).

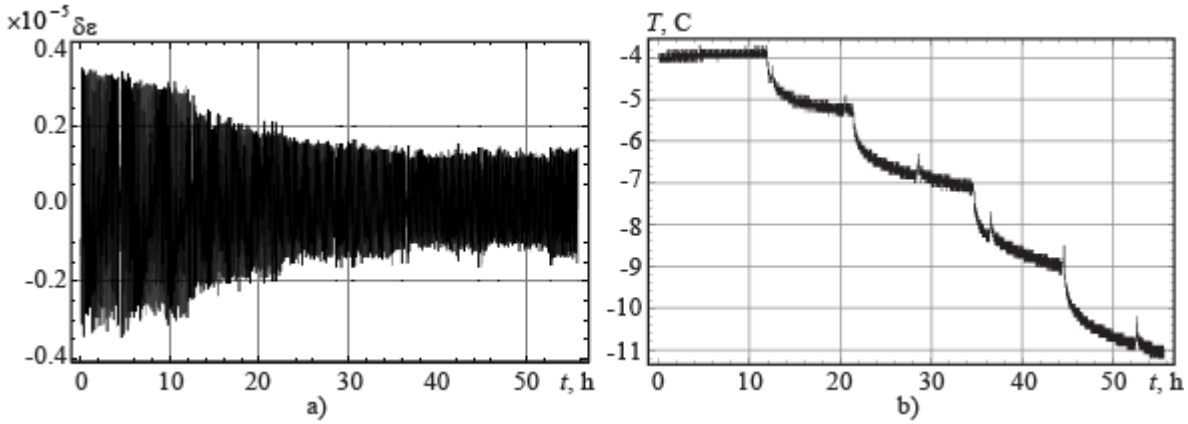

Figure 4. Oscillating part of strain $\delta\varepsilon$ (a) and the background temperature (b) versus the time.

The mean air temperature was kept the same for 5-6 hours to get stable ice temperatures several centimeters below the ice surface, and stable amplitude of thermo-elastic waves at constant mean

air temperature. The amplitude of the temperature oscillations measured in the air was 1.8°C, across a range of mean temperatures. Each experiment lasted more than 50 hours. During this time the total strain consisted of a sum of the mean strain $\langle \varepsilon \rangle$ reflecting the changes of the mean temperature in the cold laboratory (background temperature) and the strain $\delta\varepsilon$ oscillating with 12 minute period. This oscillating strain is driven by the oscillations of the background temperature in the laboratory, which arises from the laboratory's temperature control system (fans are switched on and off automatically, on a 12 minutes cycle, to maintain the mean temperature). A moving average was applied to extract the trend of the total strain. Figure 4a shows an example of the oscillating strain and the background temperature recorded over 56 hours in an experiment with an ice torus of 6 ppt salinity. The general trend of the strain amplitude $A_{\delta\varepsilon}$ is clearly visible: the strain amplitude decreases with decreasing mean background temperature.

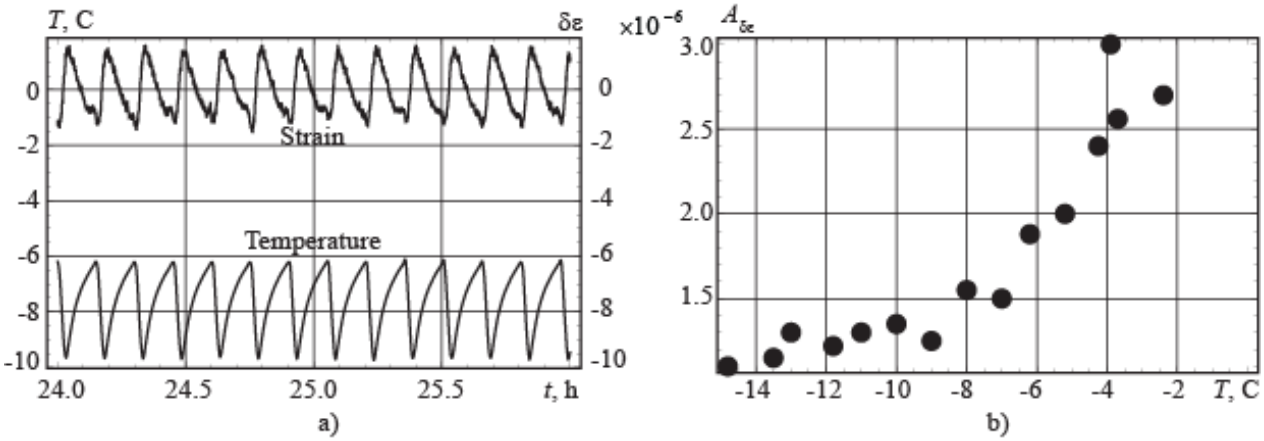

Figure 5. Zoomed dependence of the strain and background temperature oscillations on time (a). The amplitude of strain oscillations versus the mean background temperature (b).

Figure 5 shows zoomed dependence of the strain and the background temperature on time. Strain maxima coincide in Fig. 5a with the temperature minima. According to formula (19) this occurs when a part of the liquid brine is trapped in closed pockets. The dependence of the strain amplitude on the background temperature shown in Fig.5b is similar to the theoretical dependence shown in Fig.1b and derived for the case when a part of liquid brine is trapped in closed brine pockets. The amplitude of vertical displacements of the ice surface A_u is expressed by the formula

$$A_u = A_{\delta\varepsilon} L \,, \qquad [20]$$

where L=25 cm is the vertical dimension of the ice torus. Therefore A_u=2.5μm and $|A_u/A_T|$=1.4 μm·K^{-1}, when $A_{\delta\varepsilon}$=1 μstrain and A_T=1.8 K. From Fig. 5b it follows that $|A_u/A_T|$ increases from 1.4 μm·K^{-1} to 4.2 μm·K^{-1} when the background temperature increases from -15C to -2 C. Therefore the absolute values of the DT ratios observed in the experiment are smaller than the DT ratios shown in Fig. 1b. This is because only a part of the liquid brine is contained in the closed brine pockets.

Let us assume that all liquid brine is located in closed brine pockets at T=-8 C in saline ice of 6 ppt salinity (σ_{icp}=0.006). The theoretical value of the DT ratio is 1.4 μm·K^{-1} and the experimental

data show a DT ratio of 1.5-1.6 μm·K^{-1}. The experimental data show the increase of the DR ratio to 4.2 μm·K^{-1} when the background temperature increases to -2 C. Formula (17) gives the DT ratio 4.2 μm·K^{-1} when σ_{icp}≈0.003 at T=-2 C.

5. Conclusions

A structural model of saline ice is formulated based on the assumption that liquid brine is partially trapped in close brine pockets and partially located in permeable brine channels. It is shown theoretically that characteristics of thermo-elastic waves excited near the surface of saline ice by oscillations of the ice surface temperature depend on the amount of liquid brine trapped in closed pockets. To test this theory, we measure strain oscillations in a toroidal ice sample, caused by periodical oscillations of the background temperature. The measured dependence of ice strain amplitudes on the background temperature was found similar to the theoretical dependence of the amplitude of thermo-elastic waves excited at the surface of half-infinite layer of saline ice by periodical changes of the surface temperature on the mean temperature. Theoretical analysis shows that the observed dependence corresponds to the theory when some fraction of the liquid brine is trapped in closed brine pockets. An experiment with initial ice salinity 6 ppt demonstrates that the amount of liquid brine trapped in closed pockets decreases with increasing background temperature. In the case when all liquid brine is trapped in closed pockets at initial temperature -8 C, the salinity of the closed brine pockets drops to 3 ppt when the background temperature increases up to -2C.

Acknowledgments

The authors wish to acknowledge the support of the Research Council of Norway through the Center for Sustainable Arctic Marine and Coastal Technology (SAMCoT)

References

Cox, G.F.N. 1983. Thermal expansion of saline ice. *J. Glaciology*, 29(103), 425-432.

Johnson J.B., Metzner R.C. 1990. Thermal expansion coefficients for sea ice. *J.Glaciology*, 36(124), 343-349.

Golden, K.M., Eicken, H., Heaton, A.L., Miner, J., Pringle, D.J., Zhu, J. 2007. Thermal evolution of permeability and microstructure in sea ice. *Geoph. Res. Letters*, 34, L 16501.

Landau, L.D., Lifshitz, E.M., 1987. Fluid Mechanics 2nd edition, Elsevier, Amsterdam, 540 pp.

Malmgren, F. 1927. On the properties of sea ice. The Norwegian North Polar Expedition with the ”Maud”, 1918-1925, 1(5).

Marchenko, A., Lishman, B. 2015. Properties of thermo-elastic waves in saline ice. *POAC15-164*.

Marchenko, A., Lishman, B., Wrangborg, D., Thiel. T., 2016. Thermal Expansion Measurements in Fresh and Saline Ice Using Fiber Optic Strain Gauges and Multipoint Temperature Sensors Based on Bragg Gratings. *Journal of Sensors*. Volume 2016, Article ID 5678193, 13 pp.

Petterson, O. 1883. On the properties of water and ice. In Nordenskiold, ed. Vega-expeditionens veisnskapliga iakttagelser. Bd.2. Stockholm, F. and G. Beijers Forlag, 247-323.

Schwerdtfeger, P. 1963. The thermal properties of sea ice. *J. Glaciology*, 4 (36), 789–807.

Weeks, W.F. and S.F. Ackley. 1986. The growth, structure, and properties of sea ice. In Untersteiner, N., ed. *Geophysics of sea ice*. London, etc., Plenum Press, 9–164.

Zhu, J., Jabini, A., Golden, K.M., Eicken, H., Morris, M. 2006. A network model for fluid transport through sea ice. *Annals of Glaciology*, 44, 129-133.